

## (C<sub>2</sub>H<sub>5</sub>NH<sub>3</sub>)<sub>2</sub>CuCl<sub>4</sub>: A Physical System for the Experimental Investigation of Intrinsic Localized Modes

R. Lai and A. J. Sievers

*Laboratory of Atomic and Solid State Physics, Cornell University, Ithaca, New York 14853-2501*

(Received 8 January 1998)

The weak dissipation of spin waves in magnetic materials makes antiferromagnets realistic candidates for the experimental observation of intrinsic localized modes. Our molecular dynamics simulations with different antiferromagnets reveal that the lowest lying uniform spin wave mode of the antiferromagnet (C<sub>2</sub>H<sub>5</sub>NH<sub>3</sub>)<sub>2</sub>CuCl<sub>4</sub> is unstable and that it can be driven sufficiently hard with a 1 Oe cw microwave field to generate intrinsic localized spin wave modes. [S0031-9007(98)06965-8]

PACS numbers: 75.10.Hk, 46.10.+z, 75.30.Ds, 75.50.Ee

The realization that lattice discreteness can stabilize highly localized excitations in perfect nonlinear lattices is proving to be a new conceptual breakthrough in nonlinear dynamics [1,2]. Although a fairly detailed theoretical understanding of the important effects of lattice discreteness on intrinsic localized mode (ILM) existence, localization, and stability has been achieved [1,2], and a simple tabletop model has been realized [3], the best method for the generation [4,5] and detection [6] of these large-amplitude localized excitations in crystals is still an open question. The analogy between lattice vibrations and spin waves has stimulated recent theoretical studies of intrinsic localized spin wave modes (ILSMs) in semi-classical and classical magnetic models [7–13]. Owing to the soft nonlinearity of the spin-spin exchange interaction only intrinsic localized spin wave gap modes and/or resonances are allowed in a variety of antiferromagnetic systems. These ILSMs are *nontopological* and can exist in discrete lattices of any space dimension, so they should be contrasted with the continuum *topological* kink solitons which have been well studied in one-dimensional magnetic systems [14]. Since the dissipation of spin waves in magnetic materials [15,16] is usually weak compared to that of lattice vibrations in crystals, antiferromagnets appear to be realistic candidates for the experimental observation of ILMs. In this Letter we describe simulation studies for antiferromagnetic materials where intrinsic localized spin wave modes are created via modulational instability [17,18] when the uniform mode is driven with a large amplitude ac field. Layered antiferromagnets stand out as particularly noteworthy: We find that the lowest lying uniform spin wave mode of the antiferromagnet (C<sub>2</sub>H<sub>5</sub>NH<sub>3</sub>)<sub>2</sub>CuCl<sub>4</sub> is unstable, and it can be driven sufficiently hard with a laboratory cw microwave field so that intrinsic localized spin wave modes are produced. Since these ILSMs appear at lower frequencies than the uniform mode they can be identified and examined using microwave homodyne detection methods.

Previous studies of intrinsic localized spin wave modes in an antiferromagnetic chain with single-ion easy-axis anisotropy described by the Hamiltonian

$$H = 2J \sum_n \vec{S}_n \cdot \vec{S}_{n+1} - D \sum_n (S_n^z)^2, \quad (1)$$

where both the exchange constant  $J$  and the single-ion anisotropy constant  $D$  are positive, have demonstrated that they can exist in the gap below the antiferromagnetic resonance (AFMR) uniform mode frequency for any  $D > 0$ , and that the ratio of the anisotropy field to the exchange field,  $H_A/H_E$ , is a crucial parameter which determines the localization properties of these new modes [7,11,13,18]. For a specific maximum spin deviation, the larger the ratio  $H_A/H_E$ , the more strongly localized is the spin wave mode, with the mode frequency moving further into the gap. For the two standard easy axis antiferromagnets MnF<sub>2</sub> and FeF<sub>2</sub>, very different localization properties are to be expected. Because of its relatively weak anisotropy field,  $H_A/H_E = 10^{-3}$  [19], MnF<sub>2</sub> should generate broad intrinsic localized spin wave gap modes (ILSGs) on a short time scale, which would be difficult to identify in experiment due to the coexistence of extended nonlinear spin waves. On the other hand, FeF<sub>2</sub>, with a much larger anisotropy value,  $H_A/H_E = 0.345$  [16], is expected to produce strong localization on a much longer time scale, which because of the relatively large frequency shifts can be separated from the extended spin waves.

By means of molecular dynamics (MD) simulations we now estimate the ac field required to create ILSGs via the modulational instability of extended spin waves for an easy-axis antiferromagnetic chain of 256 spins with periodic boundary conditions. The parameters for the chain are chosen to match those of FeF<sub>2</sub>, which are given in Table I. Since only the ratios between parameters matter in these computer simulations we set  $D/J = 0.69$  in Eq. (1).

For a dissipative chain of classical spins in the presence of a circularly polarized driving field  $H_{ac}$  in the  $x$ - $y$  plane, the equation of motion for the  $n$ th spin can be written as

$$\frac{1}{\gamma} \frac{d\vec{S}_n}{dt} = \vec{S}_n \times \vec{H}_n^{\text{eff}} - \varepsilon \vec{S}_n \times (\vec{S}_n \times \vec{H}_n^{\text{eff}}), \quad (2)$$

where  $\gamma$  is the gyromagnetic ratio, the second term results from the Landau-Gilbert damping [19] which preserves the magnitude of individual spins, and  $\varepsilon$  is a small

TABLE I. Model Parameters for  $\text{FeF}_2$  [16] and  $(\text{C}_2\text{H}_5\text{NH}_3)_2\text{CuCl}_4$  [21].  $H_E$  is the exchange field,  $\vec{H}_A$  is the anisotropy field tensor,  $\vec{H}_{\text{dip}}^{s(d)} = \sum_n \vec{F}(n)$  [even (odd)  $n$ ] is the dipolar field tensor arising from the same (different) sublattice, and  $\omega_{\pm}(0)$  are the AFMR frequencies. Both  $\vec{H}_A$  and  $\vec{H}_{\text{dip}}^{s(d)}$  have only diagonal elements, which are listed here. All parameters are in units of oersteds.

	$H_E$	$\vec{H}_A$	$\vec{H}_{\text{dip}}^s$	$\vec{H}_{\text{dip}}^d$	$\omega_{\pm}(0)/\gamma$
$\text{FeF}_2$	$5.55 \times 10^5$	$1.91 \times 10^5$	Neglected	Neglected	$5.01 \times 10^5$
$(\text{C}_2\text{H}_5\text{NH}_3)_2\text{CuCl}_4$	829	{69, 974, 0}	{-247, 500, -253}	{75, -150, 75}	1915, 494

parameter measuring the damping strength. We confine our MD simulations here to the application of the simplest possible case: a cw source with a fixed driving frequency.

In the MD simulations the discrete equations of motion for the  $xyz$  spin components given by Eq. (2) are integrated numerically. Given an ac field strength, the driving frequency is set to a value slightly below the AFMR frequency of the uniform mode,  $\omega_{\text{AFMR}}$ . The optimal driving frequency should maximize the total energy fed into the antiferromagnetic chain so that the system attains the maximum nonlinear contribution.

Figure 1(a) shows the time evolution of the energy per spin in a chain driven by a cw ac field with fixed strength at three different frequencies. In each case the chain has the same initial configuration; that is, the spins are randomly deviated from their ground state configuration with an average spin deviation  $\langle \delta S_n \rangle = 0.005$ . The time is measured in units of  $T_{\text{AFMR}} = 2\pi/\omega_{\text{AFMR}}$ . These three MD simulations demonstrate that the driving frequency is a crucial parameter and that  $\omega_{\text{ac}} = 0.995\omega_{\text{AFMR}}$  is the optimal driving frequency for this particular ac field strength. For this optimal case, the energy in the chain increases smoothly with time during the first  $240 T_{\text{AFMR}}$ , and then becomes saturated at longer times with the deviations produced by irregular fluctuations. Although the details of the MD simulation results depend on the initial spin configuration, the evolution of energy per spin does not show a qualitative difference between what is shown here and other random initial configurations.

The behavior of the energy per spin in the analog  $\text{FeF}_2$  system can be understood better by examining the time evolution of the energy density distribution [11] plotted in Fig. 1(b) for the optimal case of  $H_{\text{ac}} = 4.0 \times 10^{-4}\omega_{\text{AFMR}}/\gamma$  and  $\omega_{\text{ac}} = 0.995\omega_{\text{AFMR}}$ . After the driving field is turned on the energy density distribution increases smoothly with time and remains plane wavelike, until the instability triggered by the random initial condition begins to manifest itself after about  $240 T_{\text{AFMR}}$ . With further development of the instability the extended  $q = 0$  spin wave decays into a few ILSG excitations which slowly move around the lattice. Since the ILSG excitations have lower frequencies than the uniform mode, their coupling to the ac driving field is weak and the energy in the chain reaches this steady state.

Although these numerical simulations demonstrate that the ILSMs can be generated in a chain with the  $\text{FeF}_2$  parameters via the modulational instability mechanism

by driving the unstable extended spin waves with a cw ac source, the optimum ac field parameter required corresponds to  $H_{\text{ac}} = 200$  Oe for a driving frequency of  $\omega_{\text{ac}} = 52.34 \text{ cm}^{-1}$ . Such intense sources do not yet exist in this frequency region. Since the localization property of an ILSM is really determined by the ratio of  $H_A/H_E$  it should be possible to apply the same method to excite ILSMs with  $H_A$  comparable to  $H_E$  but for antiferromagnets with the AFMR frequency in the GHz region. Furthermore, since the exchange field  $H_E$  would then be scaled down by a factor of 100, one would expect the required strength of the driving field to decrease by roughly the same factor.

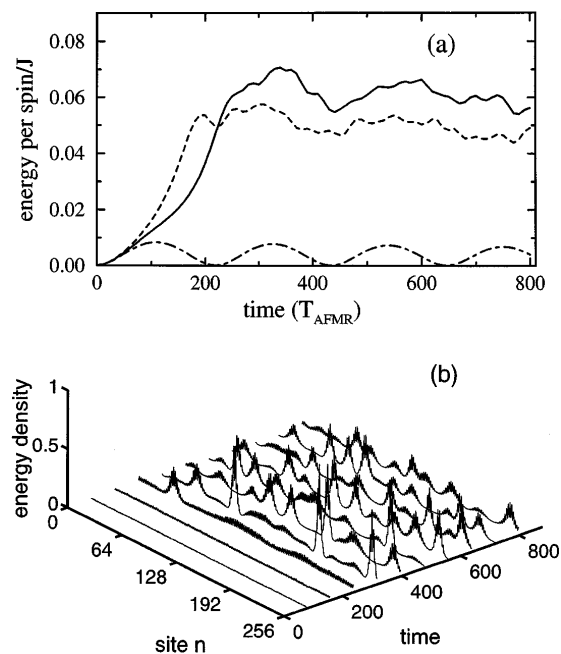


FIG. 1. Molecular dynamics simulation results of a periodic uniaxial easy-axis antiferromagnetic chain of 256 spins driven by a circularly polarized ac cw field. The parameters of the antiferromagnetic chain correspond to those of  $\text{FeF}_2$ . (a) Evolution of energy per spin for three different ac driving frequencies. The strength of the ac field is  $H_{\text{ac}} = 4.0 \times 10^{-4}\omega_{\text{AFMR}}/\gamma$ , and the frequencies of the ac cw fields  $\omega_{\text{ac}}/\omega_{\text{AFMR}}$  are as follows: 0.994 (dot-dashed line), 0.995 (solid line), and 0.996 (dashed line). (b) Energy density distribution as a function of time for the optimal driving frequency  $\omega_{\text{ac}} = 0.995\omega_{\text{AFMR}}$ . Energy density is in arbitrary units, and time is measured in units of  $T_{\text{AFMR}}$ . (The fine wiggles result from the fact that up spins for ILSGs in uniaxial easy-axis antiferromagnets have a larger deviation than adjacent down spins and hence have higher anisotropy energy [11]).

Because of these constraints we examine next a well-known quasi-two-dimensional antiferromagnet  $(\text{C}_2\text{H}_5\text{NH}_3)_2\text{CuCl}_4$  [20,21]. The structure of this compound is face centered orthorhombic. The interactions between copper ions within the  $ab$  plane are strongly ferromagnetic, and there exists a very weak antiferromagnetic interaction between neighboring copper ions in adjacent layers. At  $T = 1.4$  K the interlayer antiferromagnetic exchange field is  $H'_E = 829$  Oe, and the intralayer ferromagnetic exchange field  $H_E = 5.5 \times 10^5$  Oe. Thus  $H'_E/H_E = 1.51 \times 10^{-3} \ll 1$ , and below the Néel temperature ( $T_N = 10.2$  K) the low frequency spin dynamics can be described quite accurately by a 1D two-sublattice antiferromagnet with spins in the same layer pointing in the same direction and modeled as one effective spin.

The effective one-dimensional Hamiltonian is given by

$$H = 2J_{\text{AF}} \sum_n \vec{S}_n \cdot \vec{S}_{n+1} + \sum_n \vec{S}_n \cdot \vec{D} \cdot \vec{S}_n + \frac{1}{2} \sum_{n,n'} \vec{S}_n \cdot \vec{F}(n-n') \cdot \vec{S}_{n'}, \quad (3)$$

where  $\vec{S}_n$  is the effective spin of the  $n$ th layer and is treated as a classical vector with unit length. The antiferromagnetic exchange constant  $J_{\text{AF}} > 0$ , and the anisotropy tensor  $\vec{D}$  arises from the anisotropic ferromagnetic exchange interaction between spins belonging to the same layer. The third term describes the dipole-dipole interactions, where  $\vec{F}(n-n')$  is the effective dipolar interaction tensor between spins belonging to the  $n$ th and the  $n'$ th layers, and the dipolar interaction between spins belonging to the same layer  $\vec{F}(0)$  is the strongest. The model parameters are set to be  $J_{\text{AF}} = 207$  Oe and  $\vec{D} = \text{diag}\{34.5, 487, 0\}$  Oe so that the  $z$  axis is the easy axis, and the antiferromagnetic exchange field and the anisotropy field match those measured for  $(\text{C}_2\text{H}_5\text{NH}_3)_2\text{CuCl}_4$  which are listed in Table I. The effective dipolar interaction tensor  $\vec{F}(n-n')$  can be obtained by summing contributions from spins belonging to the  $n'$ th layer. It has only diagonal elements owing to the symmetry of the lattice [21]. Since the Hamiltonian does not possess uniaxial symmetry, there are two antiferromagnetic spin wave branches  $\omega_{\pm}(q)$  with  $\omega_+(0)/\gamma = 1915$  Oe, and  $\omega_-(0)/\gamma = 494$  Oe. Because of the negative curvature of the upper dispersion curve branch at  $q = 0$ , the existence of intrinsic spin wave resonances can be ruled out [22]; however, the positive curvature of the lower branch at the zone center permits the existence of ILSGs to occur below  $\omega_-(0)$ .

To study the creation of ILSGs in this system where dipole-dipole anisotropy is important, we again apply a cw microwave field to a chain of 256 spins with a periodic boundary condition in the MD simulations. The damping parameter  $\varepsilon$  is set to be  $10^{-5}$  so that the ratio of  $\Gamma/\omega$  is of the same order as that in  $\text{FeF}_2$ . At time 0 the spins are

randomly oriented from the easy axis by a small amount with  $\langle \delta S_n \rangle = 0.005$ .

We search for the smallest driving field strength that will induce significant localization and find it to occur when  $H_{\text{ac}} = 0.987$  Oe. After a few trials, the frequency of the driving field is set to  $\omega_{\text{ac}}/\gamma = 487.5$  Oe to maximize the energy going into the chain. The MD simulation results showing the evolution of the energy density distribution for the optimal case are plotted in Fig. 2(a). The amplitude of an extended nonlinear spin wave grows smoothly for about  $70 T_{\text{AFMR}}[2\pi/\omega_-(0)]$ , while for longer times the extended mode decays into slowly moving localized excitations. MD simulations with different random initial configurations show qualitatively similar results.

The ILSGs for this anisotropic chain have a nonzero net magnetic moment,  $M_y(t) = \sum S_n^y(t)$ , in the  $y$  direction. Figure 2(b) displays the power spectrum of  $M_y(t)$  for the MD run shown in Fig. 2(a). The power spectrum is calculated from the data during the time period from 90 and  $512 T_{\text{AFMR}}$  to exclude the contribution from initial extended spin waves. The lower frequency components

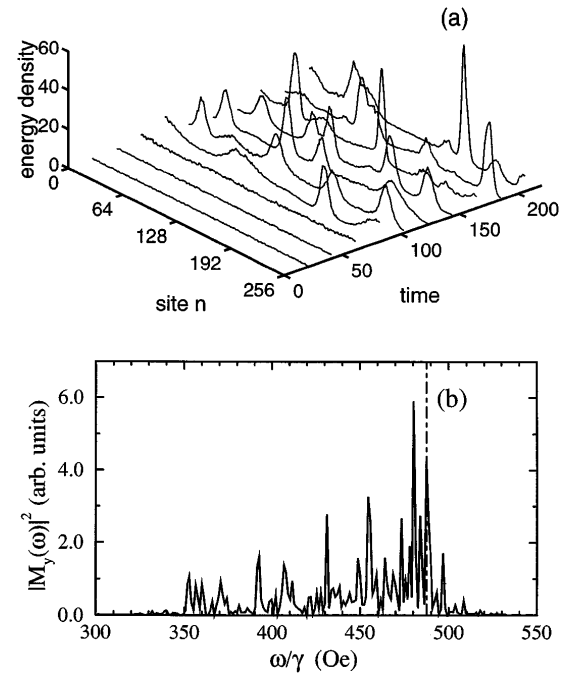


FIG. 2. Creation of intrinsic localized spin wave modes in an anisotropic antiferromagnetic chain of 256 spins driven by a circularly polarized ac cw field. The parameters of the antiferromagnetic chain correspond to those of  $(\text{C}_2\text{H}_5\text{NH}_3)_2\text{CuCl}_4$ . The frequency of the ac cw field is  $\omega_{\text{ac}}/\gamma = 487.5$  Oe, which is the optimal frequency corresponding to the applied ac field strength  $H_{\text{ac}} = 0.987$  Oe. (a) Energy density distribution as a function of time. Energy density is in arbitrary units, and time is measured in units of  $T_{\text{AFMR}}[2\pi/\omega_-(0)]$ . (b) Power spectrum of the net magnetic moment  $M_y(t)$  for the simulation run shown in (a), which is calculated from the simulation data during the time period from 90 to  $512 T_{\text{AFMR}}$ . The dot-dashed line identifies the driving frequency.

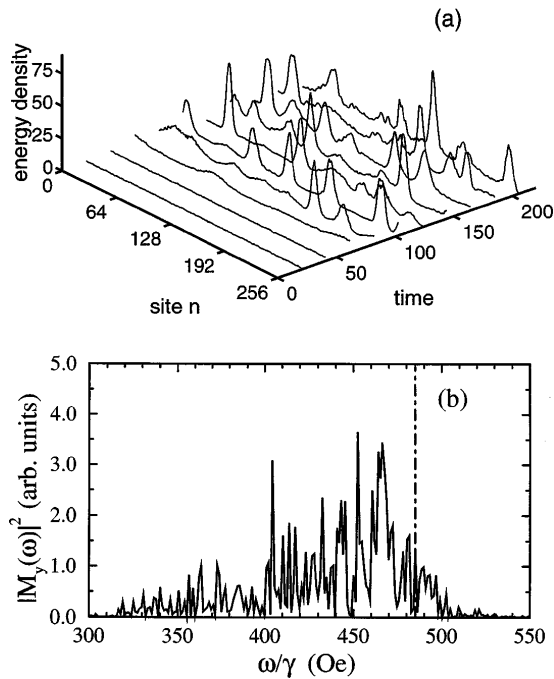


FIG. 3. Creation of intrinsic localized spin wave modes in an anisotropic antiferromagnetic chain. All parameters are the same as those in Fig. 2 except that the frequency of the ac cw field is  $\omega_{ac}/\gamma = 485$  Oe, which is the optimal frequency corresponding to the applied ac field strength  $H_{ac} = 1.396$  Oe. (a) Energy density distribution as a function of time. Energy density is in arbitrary units, and time is measured in units of  $T_{AFMR}$ . (b) Power spectrum of the net magnetic moment  $M_y(t)$  for the simulation run shown in (a). The dot-dashed line identifies the driving frequency.

shown here are generated by the ILSMs produced by the decay of unstable extended spin waves.

To demonstrate the effect of the ac field strength on the ILSG spectrum, we double the power of the cw microwave source so that the ac field strength is increased by a factor of  $\sqrt{2}$  to  $H_{ac} = 1.396$  Oe. As a consequence of the redshift resulting from the increasing driving power, the optimal driving frequency is moved down further to  $\omega_{ac}/\gamma = 485$  Oe. Figure 3 shows the MD simulation results. As plotted in Fig. 3(a), the effect of the instability begins to show up earlier owing to the increase in the driving field strength, and the ILSGs are more localized with the FWHM of the central peak of the energy-energy correlation function [18] averaged between 100 and 200  $T_{AFMR}$  equal to 17.8 compared to 20.8 in Fig. 2. The power spectrum of  $M_y(t)$  for the corresponding run is displayed in Fig. 3(b). Compared to Fig. 2(b) where the shift of the center of gravity of the frequency spectrum from the driving frequency is 9% in Fig. 3(b) there are more low frequency components producing a corresponding shift of 10% since on the average the ILSGs generated in this case have larger amplitudes and hence lower mode frequencies.

In contrast to the broad ( $\sim 1$  mm width) spin wave envelope solitons observed in yttrium iron garnet (YIG)

films [23], the spatial size of an ILSM in an antiferromagnet is comparable to the lattice spacing, and its formation and stability are strongly affected by the strength of the on-site anisotropy field and the discreteness of the underlying lattice. Since the ILSMs have frequencies below the extended spin waves and are magnetic dipole active, their signature can be directly probed by microwave homodyne detection methods.

This work is supported in part by NSF-DMR-9631298 and ARO-DAAH04-96-1-0029. Some of this research was conducted using the resources of the Cornell Theory Center.

- [1] A. J. Sievers and J. B. Page, in *Dynamical Properties of Solids*, edited by G. K. Horton and A. A. Maradudin (North-Holland, Amsterdam, 1995), Vol. 7, p. 137.
- [2] S. Flach and C. R. Willis, *Phys. Rep.* **295**, 181 (1998).
- [3] F. M. Russell, Y. Zolotaryuk, and J. C. Eilbeck, *Phys. Rev. B* **55**, 6304 (1997).
- [4] T. Rössler and J. B. Page, *Phys. Rev. Lett.* **78**, 1287 (1997).
- [5] V. M. Burlakov, *Phys. Rev. Lett.* **80**, 3988 (1998).
- [6] G. P. Tsironis and S. Aubry, *Phys. Rev. Lett.* **77**, 5225 (1996).
- [7] S. Takeno and K. Kawasaki, *Phys. Rev. B* **45**, R5083 (1992).
- [8] S. Takeno and K. Kawasaki, *J. Phys. Soc. Jpn.* **63**, 1928 (1994).
- [9] R. F. Wallis, D. L. Mills, and A. D. Boardman, *Phys. Rev. B* **52**, R3828 (1995).
- [10] S. Rakhmanova and D. L. Mills, *Phys. Rev. B* **54**, 9225 (1996).
- [11] R. Lai, S. A. Kiselev, and A. J. Sievers, *Phys. Rev. B* **54**, R12 665 (1996).
- [12] R. Lai, S. A. Kiselev, and A. J. Sievers, *Phys. Rev. B* **56**, 5345 (1997).
- [13] J. Ohishi, M. Kubota, K. Kawasaki, and S. Takeno, *Phys. Rev. B* **55**, 8812 (1997).
- [14] H.-J. Mikeska and M. Steiner, *Adv. Phys.* **40**, 191 (1991).
- [15] J. P. Kotthaus and V. Jaccarino, *Phys. Rev. Lett.* **28**, 1649 (1972).
- [16] R. W. Sanders, R. M. Belanger, M. Motokawa, V. Jaccarino, and S. M. Rezende, *Phys. Rev. B* **23**, 1190 (1981).
- [17] Y. S. Kivshar and M. Peyrard, *Phys. Rev. A* **46**, 3198 (1992).
- [18] R. Lai and A. J. Sievers, *Phys. Rev. B* **57**, 3433 (1998).
- [19] A. H. Morrish, *The Physical Principles of Magnetism* (Wiley, New York, 1965), p. 623.
- [20] J. Shi, H. Yamazaki, and M. Mino, *J. Phys. Soc. Jpn.* **57**, 3580 (1988).
- [21] M. Chikamatsu, M. Tanaka, and H. Yamazaki, *J. Phys. Soc. Jpn.* **50**, 2876 (1981).
- [22] R. Lai and A. J. Sievers, *Phys. Rev. B* **55**, R11 937 (1997).
- [23] A. N. Slavin, B. A. Kalinikos, and N. G. Kovshikov, in *Nonlinear Phenomena and Chaos in Magnetic Materials*, edited by P. E. Wigen (World Scientific, Singapore, 1994), p. 209.